

Transient Stability Indices for Fast Contingency Ranking in Large Electric Power Systems

Stefano Massucco, Federico Silvestro – University of Genoa

Emanuele Ciapessoni, Diego Cirio, Andrea Pitto – Ricerca sul Sistema Energetico RSE S.p.A.

Abstract— *The liberalization of the electricity market and the growing contribution of renewable resources RES induce a large variety of scenarios that may lead power systems close to their operation limits. On-line Dynamic Security Assessment (DSA) of the grids is thus required, in order to provide operators with a clear insight of the current network state. The on-line application of DSA to a realistic network needs adequate methods to screen the large amount of contingencies to be examined by DSA tools. This paper proposes some practical heuristic indices for Transient Stability contingency pre-filtering and ranking in an on-line DSA session. The application of the indices to an IEEE test system and to a large realistic power system gives promising results.*

Index Terms— **Dynamic Security Assessment, Contingency Screening and Ranking Methods, Power Systems, Transient Stability Assessment**

I. INTRODUCTION

Dynamic Security Assessment (DSA) [1] usually concerns TSA (Transient Stability Assessment) and VSA (Voltage Stability Assessment). VSA can be studied by Quasi Steady-State (QSS) methods [2], whereas TSA, [3]-[8], is usually carried out by three approaches: a) Time-Domain (T-D) simulation based methods, accurate, but time-consuming; b) direct methods [3], which are quick, but inaccurate; c) hybrid methods which collect the advantages of the two aforementioned methods, [4]-[6]. Hybrid method in [4] transforms the trajectories of a multi-machine power system provided by a time-domain program into the trajectory of a One-Machine-Infinite-Bus (OMIB) equivalent. At each time step of the time-domain simulator the OMIB parameters are refreshed in order to accurately assess the transient stability of the equivalent. To identify the modes of separation of the system machines, the method [4] considers their post-fault swing curves computed via a time-domain program; at each step of this program, it sorts the machines in decreasing order of their rotor angles, identifies the very first largest angular deviations (largest gaps) between any two adjacent machines thus sorted, considers as candidate *critical clusters* those which are “above these largest gaps” and computes the corresponding candidate OMIB’s parameters. The procedure is stopped as soon as a candidate OMIB reaches its unstable conditions. The adopted method is derived from the Equal-Area Criterion (EAC) which allows to determine the *Critical Machines* and to compute stability margins. Hybrid methods allow to carry out quick evaluation of TSA and to preserve a good accuracy of the models for the

grid components. However it is still useful to maintain a phase of contingency pre-filtering to avoid wasting a large amount of time for the security assessment of very stable contingencies. This time may be better used to test preventive or corrective control actions. This is even more important for those TSA tools based on heuristic approaches and pure T-D simulations, because each of the stable contingencies, which represent the majority of the contingency set, needs a simulation time usually longer than for an unstable case, as termination algorithms speed up the simulation of unstable contingencies. To this aim, some indices for contingency ranking have been proposed in literature [9]-[10]. However, they often require the T-D simulation for a significant interval after the fault clearance and they also need the calculation of both the kinetic and the potential energy of the power system. The calculation of the potential energy in turn is usually strongly based on simplified modelling assumptions. Thus, some contingency screening indexes relying only on kinetic energy have been proposed in literature [11]-[12]. This paper aims at giving a contribution to the contingency pre-filtering and ranking process during a TSA session in an on-line DSA application. To this aim it proposes a few heuristic indexes for the identification of the most advanced (critical) machines which go out of step in unstable contingencies and a kinetic energy based index for the severity ranking of the contingencies. The paper is organised as follows: Section II presents the proposed indexes. Section III describes the methodology used to evaluate the performance of the indexes. Some results of the application of the indexes to an IEEE test system and a large realistic power system are illustrated in Section IV. Some conclusions are drawn in Section V.

II. PROPOSED INDICES FOR TSA

Some practical indices for fast transient instability detection are proposed in this section: a) individual indices; b) global indices.

A. Individual Transient Instability (ITI) indices

The individual indices are calculated for each machine in the grid. When they are compared with one another, they indicate the (potentially) critical set of machines and the critical machine (the most advanced of the machines belonging to the critical set that is the machine which first goes out of step). They are useful to determine a preventive redispatching of the injected active powers from the critical machines to the non-critical ones. The procedure for the identification of the

critical set/machine is the following: 1) at first, the values of the indices for all the machines are calculated; 2) these values are put in a descending order; 3) the differences among subsequent terms are calculated. The largest gap between two indices separates the “critical” set of machines from the non-critical one. The former is composed by the machines with the values of their individual indices above the largest gap. Fig. 1 schematizes the selection algorithm of the “critical set”.

Three practical indices have been proposed:

$$ITI_1 = \frac{P_{0i}^R}{S_{fault_i}^R} \times \left(\frac{V_{fault_i}}{V_{0i}} \right)^2 \times |\Delta V_i| \times |\Delta \omega_i| \quad (1)$$

$$ITI_2 = \frac{P_{0i}^{mach}}{V_{0i}} \times |\Delta V_i| \times |\Delta \omega_i| \quad (2)$$

$$ITI_3 = |\Delta \varpi_i| \quad (3)$$

The meaning of the symbols is explained in Appendix A.

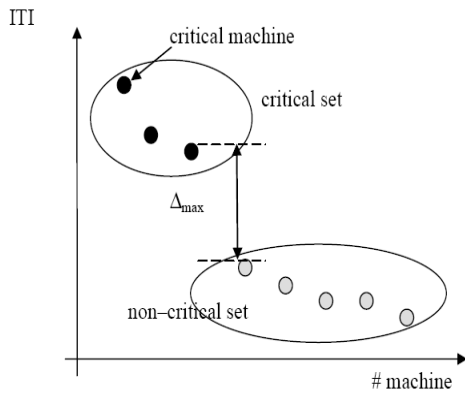


Fig. 1: Scheme of the Selection Algorithm for the Critical Set

The first index has been obtained by aggregating different quantities assumed to be interesting for TSA problem identification, such as the initial active power, the apparent power injected by each machine, the voltage and speed deviation immediately after the fault application. The tuning of the relevant exponents for each component of ITI_1 has been carried out by a “trial and error” approach. The second individual index ITI_2 indicates that the most critical machines have high initial power injections, low initial voltage and high fault-on increase of speed. Assuming the same simulation time step Δt , according to the third individual index ITI_3 the most critical machines have the highest initial acceleration with respect to the Center of Inertia (COI) which is defined in Appendix A and consists in a weighted average of the generator speeds with generator inertias acting as weights. The identification of the critical set can be used to preventively redispatch the injected active powers from the machines of the critical set to the non-critical machines. Some intuitive guidelines to actuate the preventive shift of generation from the machines of the critical set to the non-critical set are the following [4]:

- Equally from all the machines of the critical set;

- Proportionally to the nominal power of the respective machine of the critical set;
- Proportionally to their respective inertia.

Similar methods can be adopted to reallocate generation to non-critical machines, but experience [4] shows that this reallocation marginally affects transient stability.

B. Global Transient Instability (GTI) indices

The Global Transient Instability (GTI) index is aimed at identifying the most critical contingencies to be further examined in an in-depth analysis, starting from an initial set of plausible contingencies (e.g. N-1 line contingencies). As previously recalled, the conventional ranking indexes often require the T-D simulation for a significant interval after the fault clearance and they also need the calculation of both the kinetic and the potential energy which is evaluated considering simplified modelling assumptions. On the contrary, the global heuristic index proposed in this paper is based on the following observation inferred from an extended simulation experience [11]-[12]: in a stable contingency the value of the system kinetic energy E_k at the fault clearing time t_{cl} (E_{k_cl}) is lower than in an unstable contingency and the absolute value of the relative time derivative of E_k at $t = t_{cl} + \Delta t$ (i.e. $|\dot{E}_{k_pf}|/E_{k_cl}$) is higher than in an unstable contingency.

Thus, the proposed GTI index, named Kinetic Energy based Transient Instability index, is:

$$KETI = \frac{E_{k_cl}}{\left| \frac{\dot{E}_{k_pf}}{E_{k_cl}} \right|} = \frac{E_{k_cl}^2}{\left| \dot{E}_{k_pf} \right|} \quad (4)$$

The meaning of the symbols is explained in Appendix. The added value of this index is that it only needs the T-D simulation of the system behaviour until the time instant $t_{cl} + \Delta t$, immediately after the fault clearing. Another interesting peculiarity of the present index with respect to conventional ranking indexes is that it concentrates on the kinetic energy which can be easily evaluated without simplified modelling assumptions.

III. INDICES VALIDATION METHODOLOGY

A. Test systems and simulation tools

The validation of the indices has required the simulation by a T-D simulator of large set of contingencies both on simple test networks and on large power systems. As a preliminary investigation, an IEEE test system has been analyzed within a tool for power system simulation in the MATLAB environment, named PST [13]. The simulations on this test system are aimed at setting up the individual indices and the global index and at identifying the most promising individual index which is then used for the analysis of the model of a large realistic network. In particular, the simulation of a realistic model of the HV Italian transmission grid has been

carried out by means of a T-D simulator suitable for large power systems. Both simulators have been linked to a platform developed in Matlab, aimed to integrate security assessment functions and easily prototype new functions. The platform is named ISAP (Integrated Security Assessment Platform) [14]-[15]. The proposed indices have also been implemented within ISAP.

B. Proposed instability criterion

In order to evaluate the performance of the proposed indices, it is necessary to define an instability criterion used as a reference and to calculate the CCT of the examined contingencies by time domain simulations. The transient stability criterion used in time domain simulations is based on the maximum angular deviation between the rotor angle of each machine and the COI angle. This is a well-known heuristic method used in time domain simulations. The application function to identify a possible loss of synchronism calculates the COI angle of the grid:

$$\delta_{COI} = \frac{\sum_{machine\ i} [\delta_i \times M_i]}{\sum_{machine\ i} M_i} \quad (5)$$

where M_i indicates the inertia constant of machine i .

Then, the initial deviation $\Delta\delta_{COI}_0$ between the rotor angle of each machine and the COI angle is evaluated:

$$\Delta\delta_{COI}_0 = [\delta_i - \delta_{COI}]_0 \quad (6)$$

The criterion to detect instability is heuristically based on the evaluation of the maximum angular deviation, given by equation (7). When $\Delta\delta_{COI}$ reaches 360° , the function declares the loss of synchronism of the machine.

$$\Delta\delta_{COI} = \delta_i - \delta_{COI} - [\delta_i - \delta_{COI}]_0 \quad (7)$$

This check is carried out also for a reasonable time after the loss of synchronism of the most advanced machine, in order to identify also the whole (possible) set of machines which go out of step.

The instability criterion allows to find the CCT's of the contingencies of a predefined set.

C. Global Transient Instability index validation procedure

The procedure for the GTI index validation acts according to the following steps:

1. At first one clearing time CT is fixed;
2. The GTI index values are calculated for all the contingencies of the set, assuming the clearing time defined in step 1;
3. By a trial and error method the CCT (i.e. the clearing time of the marginally stable case) of each contingency is calculated; the heuristic method above is adopted to assess the loss of synchronism. This is the most time consuming phase of the procedure;

4. The contingencies are then ranked by sorting the GTI indices in descending order (thus building the "GTI-based" contingency ranking list);

5. The same contingencies are ranked by sorting the CCT's in ascending order (thus building the "CCT-based" contingency ranking list).

The factor which is calculated to evaluate the effectiveness of the GTI index is the so called "capture ratio", already used in literature [9]. If one considers the first N ranked contingencies in the CCT-based contingency ranking list and M out of N are also included in the first N elements of the GTI-based contingency ranking list, then the capture ratio of the index is given by M/N for a contingency set size equal to N.

D. Individual Transient Instability index validation procedure

ITI indices are calculated at the time instant immediately after the fault application and they are independent from the fault duration. For each contingency of the set, the procedure for ITI indices validation acts according to the following steps:

1. The contingency is simulated and the relevant ITI index values are calculated;
2. The critical set is identified through the selection algorithm illustrated in section A;
3. the contingency is simulated with a clearing time set to the marginally unstable case. The machines which go out of step are identified;
4. the sets of critical machines at steps 2 and 3 are compared.

The two validation procedures (for GTI and ITI indices) which have been separated in the paper for the sake of clarity are carried out in parallel. In fact the time-domain simulations used to identify the CCT's also provide the quantities for the calculation of the values of ITI indices and the information of the critical machines in marginally unstable cases.

IV. VALIDATION RESULTS

At first, the validation of the indices has been carried out on an IEEE test system in PST in order to set up the indices and identify the most promising ITI index. After that the GTI index and the promising ITI index have been applied to the study of a model of a large realistic power system.

A. Validation for the considered IEEE Test system

The considered test system is the IEEE 10-machine, 39-bus New England network [13], shown in Fig. 2. The analyzed contingencies consist in a zero-impedance three-phase short circuit applied near each terminal of the lines inside the grid. The fault is removed by opening the ends of the affected line. The clearing time (CT) chosen for the calculation of the GTI index values is 300 ms. The contingency set consists of 66 contingencies: in fact there are 34 lines inside the grid, but the contingencies which divide the grid into two separate parts

(i.e. the contingencies applied to line 16-19) are not considered, because the calculations hold valid for only one electric island.

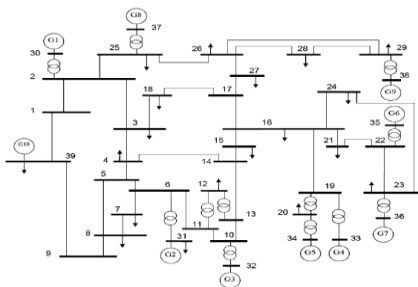


Fig. 2: IEEE Test system used for index set-up

1) ITI indices

This paragraph is aimed at comparing one another the proposed ITI indices. Only the contingencies with CCT lower than 400 ms (that is a reasonable limit for the CCT investigation) are considered.

Fig. 3 shows the estimated critical machine (blue O) by the individual index ITI_1 and the actual critical machine found by T-D simulation (black X). The blue circles represent the critical machine according to the proposed ITI index (see section A), while the black crosses indicate the machine which first goes out of step in T-D simulations.

The first proposed individual index ITI_1 has a good performance. It correctly identifies the critical machine in 36 out of 39 unstable contingencies.

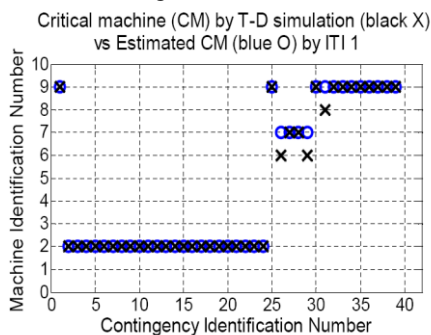


Fig. 3: Diagram of the actual critical machines (black crosses) and of the estimated critical machines by means of individual index ITI_1 (blue circles) – IEEE Test system

Fig. 4 and Fig. 5 show the same comparison in case of the other two individual indices ITI_2 and ITI_3.

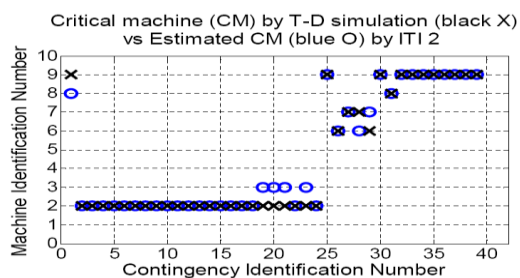


Fig. 4: Diagram of the actual critical machines (black crosses) and of the estimated critical machines by means of individual index ITI_2 (blue circles) – IEEE Test system

Critical machine (CM) by T-D simulation (black X) vs Estimated CM (blue O) by ITI 3

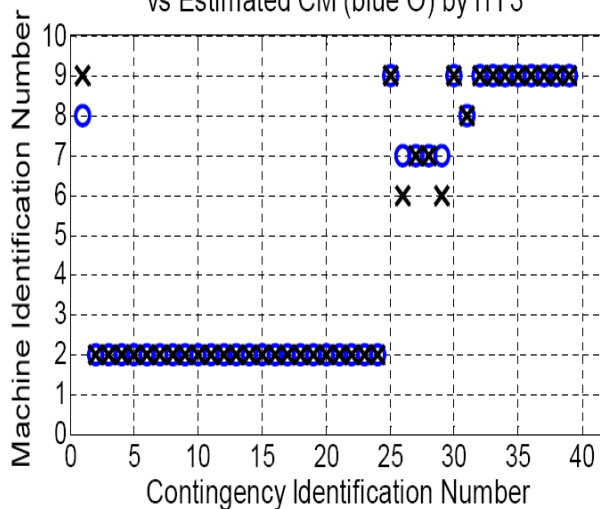


Fig. 5: Diagram of the actual critical machines (black crosses) and of the estimated critical machines by means of individual index ITI_3 (blue circles) – IEEE Test system

The best performing individual indices are ITI_1 and ITI_3. Now some comments to the estimated critical sets are proposed. In contingencies number 26 and 29, respectively associated to faults at lines 22-21 and 23-24, ITI_1 and ITI_3 seem to fail. However, the critical machine identified by ITI_1 and ITI_3 belongs to the actual critical set, obtained through time-domain simulations. Moreover the actual critical machine in contingency 29 (i.e. machine 6) belongs to the critical set identified by index ITI_1.

2) GTI index

This subsection is aimed at assessing the effectiveness of the GTI Index by comparison with the ISAP time-domain simulator: the first step consists in calculating the CCT's for all the contingencies.

Fig. 6 is a scatter plot where the y-axis shows the GTI Index values and the x-axis shows the CCT values. A decreasing trend between the values of the GTI Index and the CCT's of the analyzed contingencies is evident, at least for CCT's lower than 400 ms (a reasonable limit for the CCT investigation).

The higher the GTI the lower the CCT of the contingency. The GTI Index values are thus useful to compare the severity of the contingencies belonging to the analysis set. In fact, given the same CT for the calculation of the GTI index, the contingencies with the highest GTI index values have the lowest CCT's.

Table I shows the CCT-based severity ranking list and the GTI-based severity ranking list containing the first 20 contingencies.

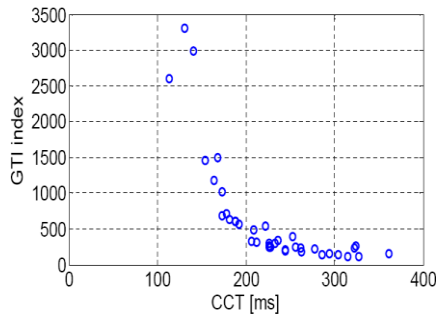


Fig. 6: Overall scatter plot between the GTI Index values and the CCT's – IEEE Test system

Table I: GTI Index -based and CCT-based severity ranking lists (IEEE Test system)

Ranking number	GTI Index	Contingency	CCT [ms]	Contingency
1	3304.90	failure29_26	113	failure29_28
2	2983.90	failure28_29	131	failure29_26
3	2596.90	failure29_28	141	failure28_29
4	1499.30	failure28_26	154	failure6_11
5	1461.80	failure6_11	164	failure6_5
6	1172.50	failure6_5	168	failure28_26
7	1021.00	failure6_7	173	failure5_4
8	713.30	failure5_6	173	failure6_7
9	687.90	failure5_4	178	failure5_6
10	638.50	failure26_29	181	failure26_29
11	602.00	failure26_28	188	failure5_8
12	599.50	failure5_8	188	failure26_28
13	565.80	failure26_25	192	failure26_25
14	541.00	failure25_2	206	failure11_6
15	487.20	failure26_27	209	failure26_27
16	391.80	failure25_26	212	failure11_10
17	345.10	failure10_13	222	failure25_2
18	335.40	failure16_17	226	failure7_6
19	326.60	failure11_6	226	failure7_8
20	318.30	failure11_10	226	failure8_9

It can be noticed that even if the order is not strictly the same in the two lists, the contingencies with the lowest CCT's (for example, failure at lines 29-28, 29-26 and 28-29) are classified in the top part of the GTI-based contingency ranking list. Fig. 7 shows the capture ratio of the GTI Index as a function of the contingency set size. The performance of the GTI index is good. It reaches a 100% effectiveness for several low values of the contingency set N (defined in section 0.C) and it always maintains a value higher than 80% also for small size contingency set.

This is even more valuable if one considers that the calculation of the proposed GTI Index requires only the simulation of the contingency in the during-the-fault period in a time domain simulator, while other indices in literature, like in [9], require also the simulation of a remarkable post-fault time interval.

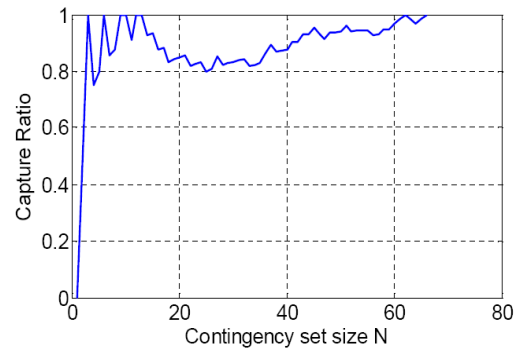


Fig. 7: Capture ratio as a function of the size of the contingency set – IEEE test system

B. Validation for the considered large power system

The realistic power system considered for this work is a historical model of the Italian HV transmission grid. The model describes the national 220 and 400 kV transmission grid and the equivalents referred to foreign countries.

The overall model includes 1471 buses, 2525 (physical) nodes, 518 generators, 1076 transformers, 1159 HV lines and 215 power plants.

GTI Index

As the GTI Index seemed promising in a small scale power system, its application to a large power system has been tested. This paragraph describes the first results obtained from the use of the GTI Index for contingency ranking purposes on the aforementioned model of the Italian HV transmission grid. In this preliminary investigation the considered contingencies refer only to 400 kV transmission lines and they consist in a zero-impedance three-phase short circuit applied in the middle of the line and cleared by opening both the terminals of the line. On one side, the DSA Manager has been used to sequentially calculate the CCT's of a set of 176 line contingencies. The upper limit for the CCT search has been set to 400 ms. After the analysis, the ISAP tool found out 65 contingencies with a CCT lower than 400 ms. As mentioned in section III.C, a fixed clearing time has to be adopted to calculate the GTI Index. Techniques for the choice of the adequate clearing time are under investigation. The simulations carried out so far demonstrate that the GTI Index maintains a good performance for a range of CT (100-250 ms) close to the typical intervention times of HV protection relays. Fig. 8 shows the influence of the CT value for the calculation of the GTI index values, by showing the capture ratio curves for three different CT. As one can notice, the performance of the index remains good for all the three considered CT values: for CT=200 ms the capture ratio is always higher than (or equal to) 80% for N larger than 9: it reaches 78.8% only once, for N=33. For CT=150 ms the GTI index first becomes higher than 80% (84.6%) for N=13; for larger values of N the values of the capture ratio are always higher than 80% (with only one exception for N=29, when the capture ratio is 79.3%).

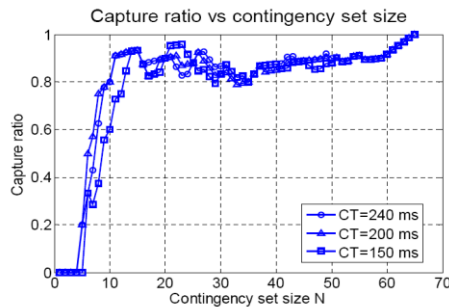


Fig. 8: Influence of the CT values adopted for the calculation of the GTI index – Italian transmission grid model

For further remarks the value of 240 ms has been considered. The proposed GTI and ITI indices have been calculated for all 176 contingencies. Then 65 contingencies with a CCT lower than 400 ms have been identified together with their relevant GTI Index values. Thus, a reduced GTI index-based contingency ranking list (based on the above mentioned 65 contingencies) has been created by sorting the selected GTI index values in descending order. Table II shows the first 20 contingencies of the CCT-based and the reduced GTI Index-based contingency ranking lists. As a further comment, the first 20 most critical contingencies in the reduced GTI index-based contingency ranking list coincide with the first 20 most critical contingencies in the complete GTI index-based list, which is a confirmation of the ranking capability of the proposed GTI index. From Table II one can notice that the GTI Index is able to classify the most critical contingencies in the top part of its contingency ranking list. The proposed GTI Index correctly captures the most dangerous contingencies, located in different areas of the system.

Table II: Reduced GTI Index-based and CCT-based contingency ranking lists (Italian transmission grid model)

Ranking number	GTI Index	Contingency	CCT [ms]	Contingency
1	5565.20	NN1345	87	NN1348
2	4241.50	NN1350	87	NN1349
3	2797.20	NN1352	99	NN1321
4	2468.00	NN1343	104	NN1353
5	2139.80	NN1353	116	NN1320
6	1982.50	NN1320	118	NN1324
7	1961.50	NN1348	119	NN1319
8	1961.50	NN1349	133	NN1343
9	1935.50	NN1324	136	NN1352
10	1832.50	PP1339	150	NN1350
11	1831.00	NN1319	157	NN1345
12	1822.00	NN1351	192	NN1351
13	1656.10	NN1318	194	NN1318
14	1654.80	NN1321	218	NN1330
15	1471.90	RR1309	222	PP1339
16	1471.90	RR1310	224	NR1355
17	1167.00	NN1330	227	MM1382
18	1088.30	NN1331	241	RR1309
19	1062.00	NN1358	241	RR1310
20	1020.30	RR1311	246	NN1331

Fig. 9 shows the capture ratio as a function of the size N of the contingency set.

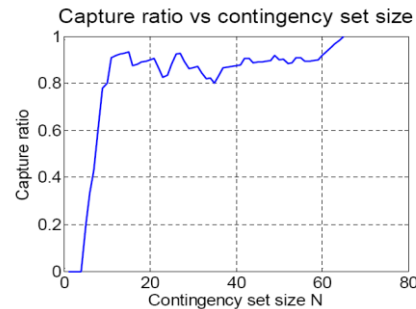


Fig. 9: Capture Ratio As A Function Of The Contingency Set Size – Italian Transmission Grid Model

The capture ratio already performs well for contingency set sizes between 10 and 20. At N=11 the capture ratio is 91% and already at N=8 it is equal to 63%. Globally the performance can be considered good because the capture ratio is always higher than 80% for N larger than 9.

Individual index ITI 1

Another objective of the analysis consists in evaluating the performance of the individual index ITI_1 in identifying the critical machines. For all the 65 contingencies with a CCT lower than 400 ms the procedure provides information about the machines which go out of step during the time domain simulation. The ITI_1 index has been calculated for all the considered 176 contingencies. For each of the 65 contingencies, column 2 of **Error! Reference source not found.** shows the machines which actually go out of step according to ISAP, column 3 and column 4 respectively show the most advanced machine of the critical set and the list of machines belonging to the critical set according to ITI_1 index. Each contingency is characterized by a “flag” variable which can assume three values (1, 2 or 3). For the contingencies with “flag” value equal to 1, the most advanced machine of the critical set indicated by index ITI_1 is also the first machine which goes out of step. The condition “flag=2” refers to the contingencies where the actual machine which first goes out of step is included in the critical set identified by index ITI_1. The other machines which go out of step are totally or partially included in the critical set by index ITI_1. At last, the condition “flag=3” refers to cases for which the prediction process fails. It can be noticed that all the machines which are signaled for loss of synchronism in the time domain simulation are included in the critical set, estimated by ITI_1, in 53 cases out of 65. In 8 out of 65 cases they are partially included inside the critical set estimated by ITI_1. In 46 cases the most advanced machine of the critical set identified by ITI_1 index is also the first machine which goes out of step. In 3 out of 65 cases, where the individual index ITI_1 seems to fail, the critical set identified by ITI_1 is (however) made up of generating units belonging to the same power plant of the critical machine signaled by ISAP.

V. CONCLUSION

The paper has proposed some Individual Indices and one Global Index for Transient Stability Assessment in power systems. The simulations carried out on an IEEE test power system show that the Individual Indices, above all ITI_1 and ITI_3, are able to identify the critical machine in almost all the unstable contingencies. The proposed Global Index, based on the kinetic energy derivative, has a good correlation with the CCT of the contingency and it allows to compare the severity of the contingencies themselves. It can be calculated by simulating only the “during fault” period in a time domain simulator. This last aspect is very important for an on-line application of this screening and ranking tool. The application of the indices to a large realistic power system has confirmed the good performance of the first Individual Index (ITI_1), which detects the most advanced machine of the critical set in most contingencies, and of the proposed Global Index (KETI) which is able to select and rank the most critical contingencies.

VI. ACKNOWLEDGMENT

This work has been financed by the Research Fund for the Italian Electrical System under the Contract Agreement between RSE and the Ministry of Economic Development - General Directorate for Energy and Mining Resources stipulated on July 29, 2009 in compliance with the Decree of March 19, 2009.

REFERENCES

- [1] CIGRE Working Group C4.601, “Review of on-line dynamic security assessment tools and techniques”, Technical Brochure 325, June 2007.
- [2] T. Van Cutsem, C. Vournas, “Voltage Stability of Electric Power Systems”, Kluwer Academic Publishers, 1998.
- [3] M. Pai, “Energy Function Analysis for Power System Stability”, Kluwer Academic Publishers, 1989.
- [4] M. Pavella, D. Ernst, D. Ruiz-Vega, “Transient Stability of Power Systems: a Unified Approach to Assessment and Control”, Kluwer Academic Publishers, 2000.
- [5] N.I. Voropai, V.G. Kurbatsky, N.V. Tomin, D.A. Panasetsky, “Preventive and emergency control of intelligent power systems,” 2012 IEEE PES Innovative Smart Grid Technologies (ISGT Europe), Berlin, Germany, Oct. 14-17, 2012.
- [6] D. Cirio, D. Ernst, D. Lucarella, S. Massucco, A. Morini, F. Silvestro, M. Pavella, G. Vimercati, L. Wehenkel, “Application of an Advanced Transient stability assessment and control method to a realistic power system”, PSCC, Liege, August 2005.
- [7] F. Saccomanno, “Electric Power Systems: Analysis and Control”, IEEE Press Series on Power Engineering, 2003, ISBN 0-471-23439-7.
- [8] P. Kundur, “Power System Stability and Control”, McGraw – Hill, New York, 1994.

- [9] A. Bose, C. Fu, “Contingency ranking based on severity indices in Dynamic Security Assessment”, IEEE Trans. On Power Systems, Vol. 14. No. 3, August 1999, pp. 980-986.
- [10] S. Grillo, S. Massucco, A. Pitto, F. Silvestro, “Indices-based Voltage Stability Monitoring of the Italian HV Transmission System”, Transmission & Distribution Conference and Exposition, New Orleans, Louisiana, USA, April 19 – 22, 2010.
- [11] T. Okuda, S. Nakagawa, S. Iwamoto, “A transient stability evaluation method based on kinetic energy of post-fault trajectories”, PSCE 2006, Atlanta, Georgia (USA), October 29 - november 1, 2006.
- [12] V. Kolluri, S. Mandal, M. Y. Vaiman, M. M. Vaiman, Member, S. Lee, P. Hirsch, “Fast Fault Screening Approach to Assessing Transient Stability in Entergy’s Power System”, IEEE PES General Meeting ‘07, Tampa, FL, June 24-28, 2007.
- [13] J. H. Chow and K.W. Cheung, “A toolbox for power system dynamics and control engineering education and research”, IEEE Transactions on Power Systems, Vol. 7, No. 4, pp.1559-1564, Nov 1992 .
- [14] E. Ciapessoni, D. Cirio, A. Pitto, S. Massucco, F. Silvestro “An Innovative Platform integrating Deterministic and Probabilistic tools for Power System Security Assessment within a Unified Approach”, 2nd IEEE- International Energy Conference and Exhibition (EnergyCon2012), Florence, September 9 – 12, 2012, ISBN: 978-1-4673-1454-12.
- [15] E. Ciapessoni, D. Cirio, S. Grillo, S. Massucco, A. Pitto, F. Silvestro, “Operational Risk Assessment and control: A probabilistic approach”, 2010 IEEE PES Innovative Smart Grid Technologies Conference Europe (ISGT Europe), Goteborg, Sweden, Oct 11-13, 2010.

AUTHOR’S PROFILE

Emanuele Ciapessoni graduated in Physics and Ph.D. in Computer Science at University of Milan. He joined CISE in 1990 and currently he is Leading Scientist in “Ricerca sul Sistema Energetico S.p.A.” (RSE, formerly ERSE, CESI RICERCA) in the Power Systems Development department. His research activities concern distributed automation, defense and risk evaluation of power systems. He participated, also as coordinator, in several national and international UE Projects dealing with PS automation. Convenor of Italian Electrotechnical Committee (CEI) WG on functional safety of systems, he serves as Italian delegate of IEC TC 65 on security and safety of control and protection systems. He has published over 60 scientific papers and reports on PS automation and he has been referee and chair in several international conferences about automation.

Diego Cirio (IEEE SM ‘13) received the M.Sc. degree (1999) and Ph.D. degree (2003) in Electrical Engineering from University of Genoa, Italy. He was with CESI from 2003 to 2005, involved in studies for the Operations department of the Italian Transmission System Operator. Currently he is with “Ricerca sul Sistema Energetico - RSE S.p.A.” where he leads the Grid and Infrastructure Security research group. He is involved in national and EU research projects on power system security assessment and secure integration of renewables, HVDC grids, and probabilistic risk assessment and control, including TWENTIES, iTESLA, and AFTER. He acted as co-Operating Agent of the IEA ENARD Annex IV “Transmission systems” and is involved in IEA ISGAN Annex 6 “T&D system issues”. He contributed to the CIGRE WG C4.601 on Power system security assessment.

Stefano Massucco (IEEE M 1980-SM 2013) received the Doctor degree in electrical engineering at the University of Genoa, Italy, in 1979. From

1979 to 1987, he had been working at the Electrical Engineering Department of Genoa University, at CREL - the Electrical Research Center of ENEL (Italian Electricity Board) in Milano, Italy, and at ANSALDO S.p.A. in Genoa, Italy. He has been Associate Professor of Power Systems at the University of Pavia and since 1993 at the Electrical Engineering Department, University of Genoa, as Full Professor since 2000. His research interests are in power systems and distributed generation modelling, control, and management. Member of Working Group 601 of Study Committee C4 for "Review of on-line Dynamic Security Assessment Tools and Techniques".

Andrea Pitto (IEEE S'06-M'10) was born in Genoa on March 2, 1981. He received his Doctor degree in Electrical Engineering from the University of Genoa, Italy, in 2005, and a PhD in Electrical Engineering from the same university in 2009 with a thesis on deterministic and probabilistic approaches to power system security assessment. He worked as a research assistant at the Naval and Electrical Engineering Dept, Genoa University, in the period 2009-2010. He joined RSE in January 2011. His area of interest includes probabilistic and deterministic approaches to power system security assessment modelling and control of distributed generation, and of HVDC transmission systems for off-shore wind power integration, application of bifurcation theory techniques to power systems analysis.

Federico Silvestro (IEEE S'01-M'03) was born in Genoa, Italy, in 1973. He received the electrical engineering degree and the Ph.D. degree in electric power systems from the University of Genoa in 1998 and 2002, respectively.

He is currently Assistant Professor at DITEN, University of Genoa. He is an author of more than 80 scientific papers. His current research interests include distributed generation and smartgrids, energy saving, dynamic security assessment, and knowledge-based systems applied to power systems. Dr. Silvestro is a member of the CIGRE Working Group 06 of Study Committee C19 for "Planning and Optimization of Active Distribution Systems."

APPENDIX

Appendix reports the list of symbols used in the present paper.

P_{0i}^R	initial active power injected by the i-th machine on system base
P_{0i}^{mach}	initial active power injected by the i-th machine on machine base
t_f	time instant of fault application
Δt	simulation time step
$S_{fault-i}^R$	apparent power injected by the i-th machine (on system base) at $t = t_f + \Delta t$
ΔV_i	initial p.u. voltage drop at the i-th machine terminals at $t = t_f + \Delta t$
$\Delta \omega_i$	speed variation of the i-th machine at $t = t_f + \Delta t$
V_{0i}	initial voltage at the i-th machine's terminals
$V_{fault-i}$	voltage at the i-th machine's terminals at $t = t_f + \Delta t$
M_j	inertia constant of the i-th machine
$\omega_{COI} = \sum_{i=1}^{N_g} M_i \times \omega_i / \sum_{i=1}^{N_g} M_i$	Center of Inertia (COI) speed
$\Delta \varpi_i$	initial variation of $\varpi_i = \omega_i - \omega_{COI}$
$E_{k-cl} = E_k(t_{cl}) = \sum_{j=1}^{N_g} \frac{1}{2} \cdot M_j (\varpi_j(t_{cl}))^2$	Total kinetic energy at the fault clearing time t_{cl}
$\dot{E}_{k-pf} = (E_k(t_{cl} + \Delta t) - E_k(t_{cl})) / \Delta t$	time derivative of the E_k immediately after the fault clearing

Table III: Critical Machines Identification – time domain simulation vs. ITI_1 index (Italian transmission grid model)

Contingency	Critical machines found by time domain simulation (ISAP)	Individual index ITI_1		Flag
		Critical machine	Critical set	
FF1316	PCOFG3, PCOFG4, ECRBGB, ECRBG1, ECRBG2	PCOFGG	PCOFGG, PCOFG4, ECRBGB, ECRBGA, PCOFG3, ECRBG1, ECRBG2, FSNVG4, FSNVG3	2
MM1317	OSCMGE	OSCMGE	OSCMGE	1
MM1358	SFIMG3	SFIMG3	SFIMG3, EDOMG4, EDOMG6, EDOMG8	1
MM1362	TURMG4, TURMG2	TURMG2	TURMG2, FRBAGC, TURMG4, FRBAGA, TURMG3, ROVMG8, ROVMG6, FRBAG2, CHITG1, ROVMG5, TURMG1	2
MM1378	SFIMG3	SFIMG3	SFIMG3, EDOMG4, EDOMG6, EDOMG8	1
MM1379	SFIMG3	SFIMG3	SFIMG3, EDOMG4, EDOMG6, EDOMG8	1
MM1382	FRBAG2	FRBAGC	FRBAGC, FRBAGA	3
MM1383	FRBAG2	FRBAGC	FRBAGC, FRBAGA	3
MM1903	ROVMG6	ROVMG6	ROVMG6, ROVMG8, ROVMG5	1
MM1935	TURMG2	TURMG2	TURMG2, TURMG4, ROVMG8, TURMG3, ROVMG6, CHITG1, FRBAGC, FRBAGA, ROVMG5, TURMG1, FRBAG2, CHITGB, CHITGA	1
MM1936	TURMG2	TURMG2	TURMG2, TURMG4, ROVMG8, TURMG3, ROVMG6, CHITG1, FRBAGC, FRBAGA, ROVMG5, TURMG1, FRBAG2, CHITGB, CHITGA	1
MM1937	TURMG2	TURMG2	TURMG2, TURMG4, ROVMG8, TURMG3, ROVMG6, CHITG1, FRBAGC, FRBAGA, ROVMG5, TURMG1, FRBAG2, CHITGB, CHITGA	1
MM1938	TURMG2	TURMG2	TURMG2, TURMG4, ROVMG8, TURMG3, ROVMG6, CHITG1, FRBAGC, FRBAGA, ROVMG5, TURMG1, FRBAG2, CHITGB, CHITGA	1
MT1313	FRBAG2	FRBAGC	FRBAGC, FRBAGA	3
NN1313	BSCNG1, BSCNG2, BSCNG3, BSCNG4, BRNNG4	TVDRG4	TVDRG4, CAPNG2, BSCNG1, BSCNG2, BSCNG3, BSCNG4	2
NN1314	BSCNG1, BSCNG2, BSCNG3, BSCNG4, BRNNG4	BSCNG1	BSCNG1, BSCNG2, BSCNG3, BSCNG4, ROSNG2, ROSNG3, BRNNG4	1
NN1315	BSCNG1, BSCNG2, BSCNG3, BSCNG4, BRNNG4	BSCNG1	BSCNG1, BSCNG2, BSCNG3, BSCNG4	1
NN1317	BSCNG1, BSCNG2, BSCNG3, BSCNG4, BRNNG4	BSCNG1	BSCNG1, BSCNG2, BSCNG3, BSCNG4, CAPNG2, TVDRG4	1
NN1318	BSCNG1, BSCNG2, BSCNG3, BSCNG4, BRNNG4	BSCNG1	BSCNG1, BSCNG2, BSCNG3, BSCNG4, BRNNG4	1
NN1319	BSCNG1, BSCNG2, BSCNG3, BSCNG4, BRNNG4	BSCNG2	BSCNG2, BSCNG1, BSCNG3, BSCNG4, BRNNG4	2
NN1320	BSCNG1, BSCNG2, BSCNG3, BSCNG4	BSCNG2	BSCNG2, BSCNG3, BSCNG1, BSCNG4, BRNNG4	2
NN1321	BSCNG1, BSCNG2, BSCNG3, BSCNG4	BSCNG2	BSCNG2, BSCNG3, BSCNG4, BSCNG1	2
NN1322	BSCNG1, BSCNG2, BSCNG3, BSCNG4, BRNNG4	BSCNG1	BSCNG1, BSCNG2, BSCNG3, BSCNG4	1
NN1324	BSCNG1, BSCNG2, BSCNG3, BSCNG4, BRNNG4	BSCNG2	BSCNG2, BSCNG3, BSCNG1, BSCNG4, BRNNG4	2
NN1329	BSCNG1, BSCNG2, BSCNG3, BSCNG4, BRNNG4	BSCNG1	BSCNG1, BSCNG2, BSCNG3, BSCNG4, TVDRG4, CAPNG2	1
NN1330	BSCNG1, BSCNG2, BSCNG3, BSCNG4, BRNNG4	BSCNG1	BSCNG1, BSCNG2, BSCNG3, BSCNG4, BRNNG4	1
NN1331	BSCNG1, BSCNG2, BSCNG3, BSCNG4	BSCNG1	BSCNG1, BSCNG2, BSCNG3, BSCNG4	1
NN1341	BSCNG1, BSCNG2, BSCNG3, BSCNG4, BRNNG4	TVDRG4	TVDRG4	3
NN1343	BSCNG1, BSCNG2, BSCNG3, BSCNG4, BRNNG4	BSCNG2	BSCNG2, BSCNG1, BSCNG3, BSCNG4, BRNNG4	2
NN1345	BSCNG1, BSCNG2, BSCNG3, BSCNG4, BRNNG4	BSCNG2	BSCNG2, BSCNG1, BSCNG3, BSCNG4, BRNNG4	2
NN1346	BSCNG1, BSCNG2, BSCNG3, BSCNG4, BRNNG4	BSCNG1	BSCNG1, BSCNG2, BSCNG3, BSCNG4	1
NN1347	BSCNG1, BSCNG2, BSCNG3, BSCNG4, BRNNG4	BSCNG1	BSCNG1, BSCNG2, BSCNG3, BSCNG4, ROSNG2, ROSNG3, BRNNG4	1
NN1348	BSCNG2, BSCNG3, BSCNG4	BSCNG2	BSCNG2, BSCNG3, BSCNG4, BSCNG1	1
NN1349	BSCNG2, BSCNG3, BSCNG4	BSCNG2	BSCNG2, BSCNG3, BSCNG4, BSCNG1	1
NN1350	BSCNG1, BSCNG2, BSCNG3, BSCNG4, BRNNG4	BSCNG2	BSCNG2, BSCNG1, BSCNG3, BSCNG4, BRNNG4	2
NN1351	BSCNG1, BSCNG2, BSCNG3, BSCNG4, BRNNG4	BSCNG1	BSCNG1, BSCNG2, BSCNG3, BSCNG4, BRNNG4	1
NN1352	BSCNG1, BSCNG2, BSCNG3, BSCNG4	BSCNG2	BSCNG2, BSCNG1, BSCNG3, BSCNG4, BRNNG4	2
NN1353	BSCNG1, BSCNG2, BSCNG3, BSCNG4, BRNNG4	BSCNG2	BSCNG2, BSCNG1, BSCNG3, BSCNG4, BRNNG4	2
NN1357	BSCNG1, BSCNG2, BSCNG3, BSCNG4, BRNNG4	TVDRG4	TVDRG4, BSCNG1, BSCNG2, CAPNG2, BSCNG3, BSCNG4	2
NN1358	BSCNG1, BSCNG2, BSCNG3, BSCNG4, BRNNG4	BSCNG1	BSCNG1, BSCNG2, BSCNG3, BSCNG4	1
NN1367	BSCNG1, BSCNG2, BSCNG3, BSCNG4, BRNNG4	BSCNG1	BSCNG1, BSCNG2, BSCNG3, BSCNG4	1
NN1CA1	BSCNG1, BSCNG2, BSCNG3, BSCNG4, BRNNG4	BSCNG1	BSCNG1, BSCNG2, BSCNG3, BSCNG4, ROSNG2, ROSNG3, BRNNG4	1
NN1CA2	BSCNG1, BSCNG2, BSCNG3, BSCNG4, BRNNG4	BSCNG1	BSCNG1, BSCNG2, BSCNG3, BSCNG4, ROSNG2, ROSNG3, BRNNG4	1
NR1355	BSCNG1, BSCNG2, BSCNG3, BSCNG4, BRNNG4	BSCNG1	BSCNG1, BSCNG2, BSCNG3, BSCNG4	1
PP1338	SFMPG6, SFMPG5	SFMPG6	SFMPG6, SFMPG5, ISBAG2, ISBAG1, SFMPG3, ISBAGC, ISBAGA, PRGP6C	1
PP1339	ISBAG2, ISBAG1	ISBAG2	ISBAG2, ISBAG1, SFMPG6, SFMPG5, ISBAGC, ISBAGA, SFMPG3, PRGP6C	1
RR1301	TVDRG4	TVDRG4	TVDRG4	1
RR1307	TVDRG4	TVDRG4	TVDRG4, MLTRG1	1
RR1308	TVDRG4	TVDRG4	TVDRG4, MLTRG1	1
RR1309	TVDRG4	MLTRG1	MLTRG1, TVDRG4	2
RR1310	TVDRG4	MLTRG1	MLTRG1, TVDRG4	2
RR1311	TVDRG4	TVDRG4	TVDRG4, MLTRG1	1
RR1313	TVDRG4	TVDRG4	TVDRG4, MLTRG1	1
RR1314	TVDRG4	TVDRG4	TVDRG4, MLTRG1	1
RR1318	SGIRG6	SGIRG6	SGIRG6, PRVRG1, PRVRG2, MONRG2, MONRG3, MONRG1	1
RR1387	SGIRG6	SGIRG6	SGIRG6, PRVRG1, PRVRG2	1
RR1P21	SGIRG6	SGIRG6	SGIRG6, PRVRG1, PRVRG2	1
TT1356	CHITG1	CHITG1	CHITG1	1
TT1390	VDLTG3	VDLTG3	VDLTG3, VDLTG4, ETQTG1, ETQTG6, ETQTG5, ETQTG3	1
TT1392	ETQTG1	ETQTG1	ETQTG1, ETQTG6, ETQTG5, ETQTG3	1
TT1393	VDLTG3	VDLTG3	VDLTG3, VDLTG4	1
TT1395	ETQTG1	ETQTG1	ETQTG1, ETQTG6, ETQTG5, ETQTG3	1
VV1311	FSNVG4	FSNVG4	FSNVG4, FSNVG3, FSNVG1	1
VV1342	FSNVG4	FSNVG4	FSNVG4, FSNVG3	1
VV1348	FSNVG4	FSNVG4	FSNVG4, FSNVG3	1